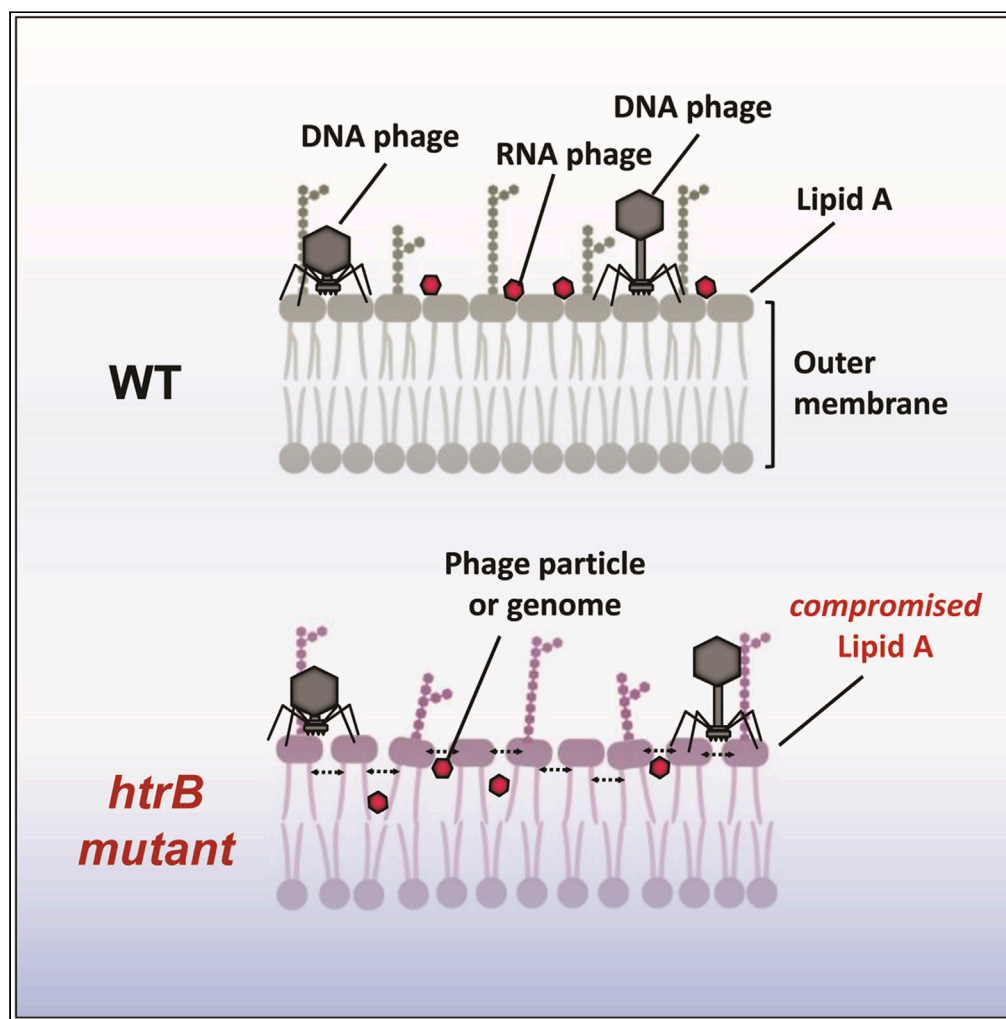**Article**

# An outer membrane determinant for RNA phage genome entry in *Pseudomonas aeruginosa*



Hee-Won Bae,
Shin-Yae Choi,
You-Hee Cho

youhee@cha.ac.kr

**Highlights**

*P. aeruginosa* mutant without lipid A secondary acyl chains is more susceptible to PP7

Loss of lipid A secondary acyl chains enhances PP7 genome entry and antibiotic uptake

Polymyxin B treatment also enhances PP7-susceptibility of *P. aeruginosa*

PP7-susceptibility is enhanced also at lower temperature (25°C) and abrogated at 42°C

### Article

# An outer membrane determinant for RNA phage genome entry in *Pseudomonas aeruginosa*

Hee-Won Bae,[1] Shin-Yae Choi,[1] and You-Hee Cho[1,2,*]

## SUMMARY

**Host range of a phage is determined at the various life cycle stages during phage infection. We reported the limited phage-receptor interaction between the RNA phage, PP7 and its host *Pseudomonas aeruginosa* strains: PAO1 has susceptible type IV pilus (TFP) pilin, whereas PA14 has resistant pilin. Here, we have created a PA14 derivative (PA14P) with the PAO1 pilin gene and found that other determinants than TFP pilin could limit PP7 infectivity in PA14P. Transposon mutant screens revealed that PP7 infectivity was restored in the PA14P mutants (*htrB2*) lacking a secondary acyltransferase in lipid A biosynthesis. The lack of this enzyme increased the RNA phage entry, which is deemed attributed to the loosened lipopolysaccharide (LPS) structure. Polymyxin B treatment also selectively increased the RNA phage entry. These results demonstrated that LPS structures could limit the entry stage of RNA phages, providing another determinant for the host range in diverse *P. aeruginosa* strains.**

## INTRODUCTION

Host range of phage is defined as the span of the bacterial hosts that allow a phage species to complete its life cycle that generally consists of five distinct steps: phage adsorption, genome entry, material synthesis, virion assembly, and phage release.[1] The host range is generally determined by the bacterial resistance mechanisms or host barriers that limit the phage infection at one of the aforementioned life cycle steps. The most common example is adsorption inhibition that is exerted by alteration, elimination, or occlusion of the phage receptors on the bacterial cell surfaces.[2] This is highly effective to prevent phage infection in that adsorption is the very first step of the phage life cycle. The second common examples are to block phage material (i.e., nucleic acids and proteins) synthesis in the bacterial cytoplasm that can occur after genome entry, as exemplified in restriction-modification and CRISPR systems that degrade the invading phage nucleic acids.[3,4] These host barriers are present in some strains of the same species and thus explain the strain-level host range of phage infection.

*Pseudomonas aeruginosa* (PA) is an opportunistic human pathogen that causes acute and chronic infections, especially in those with a compromised immune system. PA exhibits robust resistance to a wide range of antibiotics, thus prompting new antibacterial strategies to treat with, which include phage-based antibiotics or phage therapy.[5,6] Much attention has been paid to phage biology in PA by focusing on the various bacterial resistance mechanisms.[7,8] In our previous studies, superinfection exclusion was demonstrated as one of those maneuvers in some PA strains with prophages that display immunity to the related phage infection,[9,10] indicating the role of phage repressors in blockage of material synthesis. Moreover, PA strains with prophages express phage proteins that inhibits the PilB ATPase or other host proteins normally required for assembly of the well-known phage receptor, type IV pilus (TFP),[11,12] suggesting the role of phage proteins in adsorption inhibition. Recently, we first profiled the host range of a TFP-specific RNA phage, PP7, with a set of group II pilins[13] being required for PP7 infection.[14] The submolecular determinant for the PP7 host range was identified as the β1-β2 loop region of the group II pilin, which is flexibly protruding among the conserved structure of the group II pilins.[15]

In the present study, we demonstrated that the mutations for one of the HtrB/LpxL acyltransferases for lipid A biosynthesis (*htrB2*) enhanced the susceptibility to PP7, but not the TFP-specific DNA phages in the susceptible strain, PAO1. This gene was initially identified from the screen for another host barrier that restricts PP7 infection in PA14. We observed that the PP7 RNA was significantly increased in the *htrB2* mutant and that polymyxin B (PMB) affected the PP7 susceptibility by allowing more PP7 RNA genome in the cytoplasm, suggesting that the role of secondary acyl chains in lipid A as a barrier for the genome entry of the RNA phages in PA strains.

## RESULTS

### Creation of PA14P and isolation of its PP7-susceptible mutants

We previously demonstrated that the β1-β2 loop in the variable region 2 of the group II pilin might be involved in the direct interaction with the PP7 virions.[14] Introduction of the PAO1 *pilA* gene-containing plasmid (pUCP-PilA$_{PAO1}$) into the PA14 *pilA* mutant reversed the defects of the pilin mutant in twitching motility and PP7 infection, although the twitching zones and patterns were slightly different. This might be due to

[1]Department of Pharmacy, College of Pharmacy and Institute of Pharmaceutical Sciences, CHA University, Gyeonggi-do 13488, Korea
[2]Lead contact
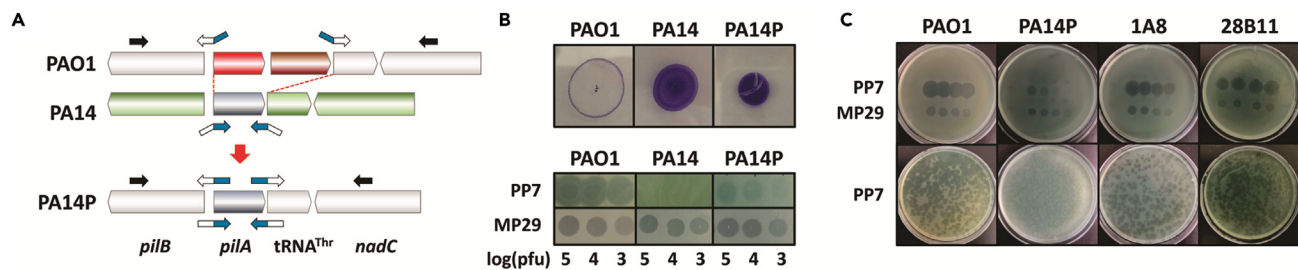*Correspondence: youhee@cha.ac.kr

**Figure 1. Creation of PA14P and isolation of its PP7-susceptible mutants**

(A) Schematic representation of the *pilA* gene region in PA14P. The *pilA* regions of the PAO1 and the PA14 genomes, both of which are flanked by the *pilB* and the tRNA^Thr genes, are represented with the primers for gene recombination schematically depicted (see Table S1).

(B) Verification of PA14P. The functionality of the *pilA* region exchange in PA14P was verified by twitching motility and TFP-specific phage susceptibility, in comparison with that in PAO1 and PA14. The twitching zones are visualized by crystal violet staining and the phage susceptibility was investigated by plaques generated by phage spots, with the numbers indicating the log (PFU) of either PP7 or MP29.

(C) Spotting and plaque phenotypes of the mutants. Phage spots from the serially 10-fold diluted phage samples of either PP7 or MP29 (upper) and PP7 plaques (lower) were investigated on the bacterial lawns of two transposon mutants (1A8 and 28B11) that had been isolated from the screening as described in method details. PAO1 and PA14P were included as the controls.

the difference in pilin group in that PA14 has an additional gene (*tfpY*) in the *pilA* gene cluster (Figure 1A). We found the plaque formation on the PA14 cells harboring pUCP-PilA_{PAO1} was not sufficiently clear, compared to that on the PAO1 cells, suggesting that PA14 might have some other host barriers than the pilin structure for PP7 infection. To clarify this issue, we have created a PA14 derivative, PA14P, whose pilin region is replaced with the corresponding region from PAO1, as depicted in Figure 1A the PA14P cells displayed the comparable twitching ability, but its susceptibility to PP7 infection was not comparable to that of PAO1 regarding plaque discernability (Figure 1B).

To identify the presumable host factors involved in the turbid plaque phenotype of the PA14 background cells, we optimized a screening procedure to identify bacterial mutants with enhanced susceptibility to PP7 infection in 96-well plate liquid culture. A total of 31,474 PA14P transposon insertion mutants were evaluated for the growth impairment only in the presence of PP7 as described in method details. Among the selected 10 clones, two clones (1A8 and 28B11) formed clear plaques on the PA14P cells (Figure 1C). This result suggests that PA14 might have a barrier for the PP7 infectivity, whose loss-of-function mutation due to transposon insertion allowed the clear plaque phenotype on the PA14P cells, apparently comparable to that on the PAO1 cells. It should be also noted that the barrier might work after the attachment step during the phage life cycle.

## Mutations in the lipid A secondary acylation enhance the RNA phage susceptibility

To identify the transposon insertion site of the 1A8 and 28B11 clones, we conducted arbitrary PCR as described previously.[16] The transposon insertions of the two clones were mapped within a gene (*htrB2* or *PA14_22050*) encoding an acyltransferase in the lipid A biosynthesis of the lipopolysaccharide outer membrane (OM) (Figure 2A). Hittle et al.[17] revealed that two acyltransferases (HtrB1 and HtrB2) are responsible for site-specific modifications of lipid A in PAO1: HtrB2 transfers secondary lauryl chain to the tetraacylated lipid A intermediate and then HtrB1 converts the pentaacylated lipid A to the hexaacylated lipid A by transferring secondary 2-hydroylauryl chain (Figure 2B). They also found that deletions of either gene enhanced the susceptibility to a set of antibiotics and especially the *htrB2* mutant showed growth defect at 25°C, likely due to the increased OM permeability and/or dysfunction of OM integrity.

Based on the known roles of two HtrB acyltransferases in the OM integrity of PA, we have created both *htrB1* and *htrB2* deletion mutants of PAO1 and PA14P strains to assess for their roles in the phage resistance. We have failed to generate the double mutant for both *htrB1* and *htrB2*, which might suggest that their critical roles in OM integrity. As shown in Figures 2C and 2D, the *htrB2*, and to the lesser extent, the *htrB1* mutants displayed more discernable plaque phenotypes on both PAO1 and PA14P cells as well as impaired growth by PP7 in liquid culture. The dramatically enhanced susceptibility of the *htrB2* mutant was observed toward PP7 infection, but not toward either MPK7 or MP29 infection, suggesting that the OM integrity directed by the lipid A secondary acylation might be critical to resist the infection by PP7. Considering the differences in virion characteristics and life cycle of the phages, we further examined the effect of *htrB* mutations on the susceptibility of another RNA phage, PRR1, that infects PAO1 via an IncP plasmid-encoded conjugative pilus.[18] Figure S1 revealed the susceptibility of PAO1 (IncP) cells to PRR1 infection was further enhanced by *htrB2* and, to the lesser extent, *htrB1*. These results lead us to the suggestion that the lipid A secondary acylation-mediated OM integrity should be a physical and/or biological barrier to the RNA phages, but not to the DNA phages.

## Lipid A acylation affects the PP7 genome entry and the antibiotic uptake

The lipid A secondary acyl chain-mediated RNA phage resistance prompted us to investigate which stage of the phage life cycle is associated with the lipid A acylation in PA strains. Since the OM is the outermost component of the Gram-negative cell wall, we first examined whether or not the phage attachment to TFP was affected by either *htrB1* or *htrB2* mutations in PAO1 and PA14P. Phage adsorption assay revealed that the adsorption rates in both *htrB1* and *htrB2* mutant bacteria (42% and 41%, respectively, for PAO1 and 40% and 41%, respectively for PA14P)
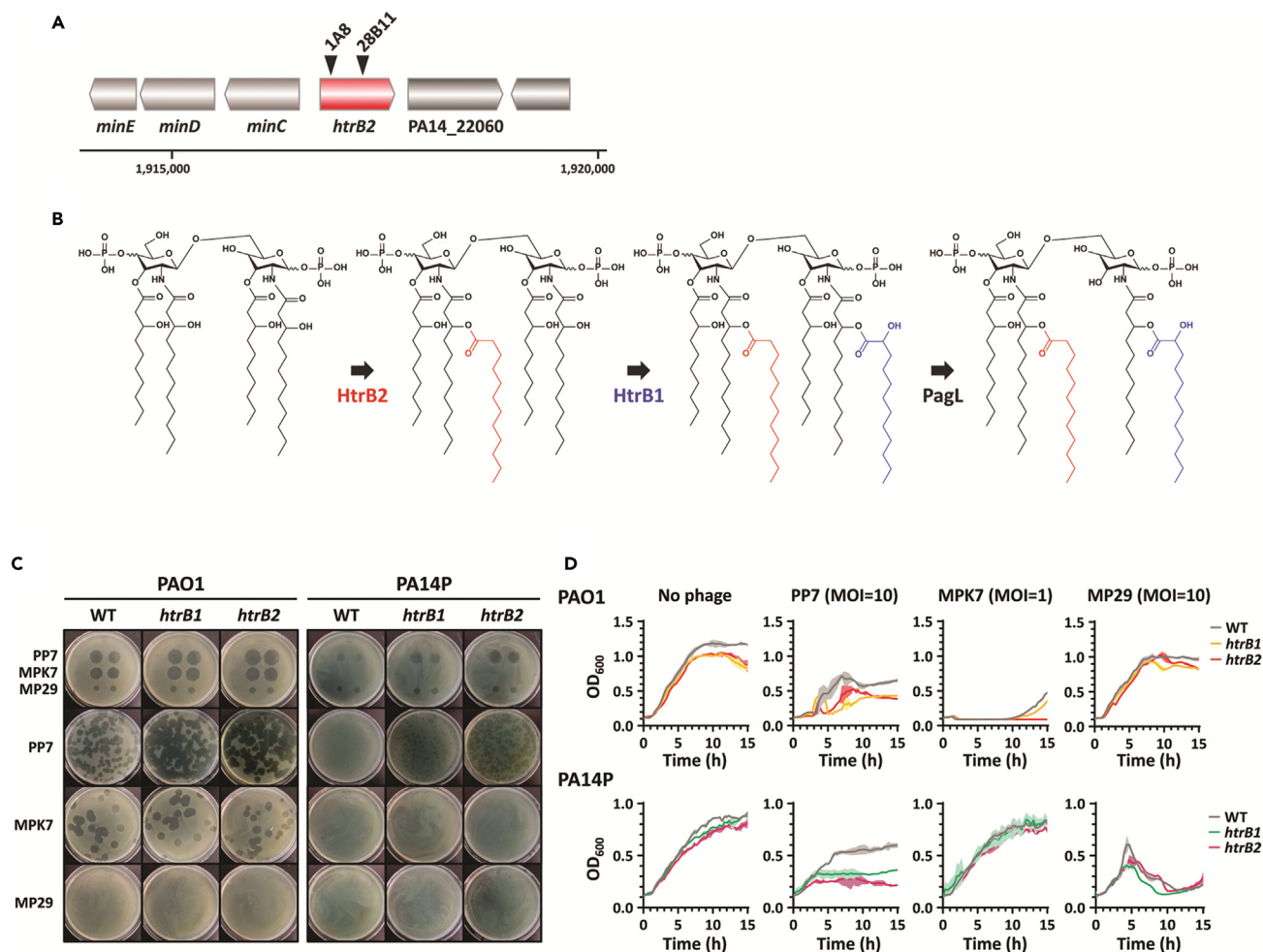
**Figure 2. HtrB2 and PP7-susceptibility**

(A) Mapping of transposon insertions in 1A8 and 28B11. Schematic representation of the genomic region containing the *htrB2* gene is shown with the PA14 genome coordinates indicated. The transposon insertion sites for 1A8 and 28B11 are designated by arrow heads in the *htrB2* gene.

(B) Role of HtrB1, HtrB2, and PagL in lipid A modification. The lipid A biosynthetic pathway in *P. aeruginosa* is partially shown, which involves HtrB1, HtrB2, and PagL enzymes for lipid A secondary acylation; HtrB2 and HtrB1 transfer a laurate and a 2-hydroxylature, respectively, to the tetraacylated lipid A; PagL removes the 3-hydroxydecanoate at the 3 position, resulting in the most abundant lipid A species in *P. aeruginosa*.

(C) Spotting and plaque phenotypes of the *htrB1* and *htrB2* deletion mutants. Phage spots from two serially 10-fold diluted phage samples of PP7, MPK7, or MP29 and their plaques were investigated on the bacterial lawns of the wild type (WT) and the isogenic mutants (*htrB1* and *htrB2*) of PAO1 (left) and PA14P (right).

(D) Growth curve of *htrB1* and *htrB2* deletion mutants at 37°C. Culture suspensions of the WT or the *htrB1* and *htrB2* mutants of PAO1 (upper) and PA14P (lower) were mixed with the phage lysates of PP7 (at MOI of 10), MPK7 (at MOI of 1), or MP29 (at MOI of 10) in LB medium and then incubated further at 37°C. The growth was assessed by measuring the $OD_{600}$ at every 20 min for 15 h.

did not differ from that in the corresponding wild-type bacteria (40% for PAO1 and 40% for PA14P) (Figure 3A). Then, we measured the steady-state levels of PP7 genomic RNA synthesis during the PP7 infection in PAO1 and PA14P strains. As assessed by RT-qPCR assay during the phage infections, the highest RNA levels were observed in the PAO1 *htrB2* and the PA14P *htrB2* mutants at 30 min post-infection, whereas slight increase in the RNA level was observed in the PA14P *htrB1* and to the lesser extent, in the PAO1 *htrB1* mutants (Figure 3B). The increase in the RNA levels was further verified by fluorescence *in situ* hybridization (FISH) to semi-quantitatively visualize PP7 genome synthesis at 30 min post-infection (Figures 3C and 3D). The FISH data agree with the RT-qPCR data in that the steady-state RNA levels during the PP7 life cycle are clearly affected by lipid A secondary acylation, which did not affect the phage adsorption at all, suggesting that the OM barrier might work after the virion attachment step, most likely at the genome entry step.

Given that the OM is implicated in antibiotic resistance of Gram-negative bacterial pathogens, working as a physical barrier to restrict chemical entry into the bacterial cells,[19,20] we tested whether the *htrB* mutations could alter the susceptibility to the previously non-permeating or weakly permeating antibiotics such as erythromycin and vancomycin.[21] As shown in Figure 4, Both *htrB1* and *htrB2* mutants were susceptible to erythromycin in PAO1 and PA14P, whereas the *htrB1* mutant was susceptible to vancomycin in PA14P, but no less susceptible in
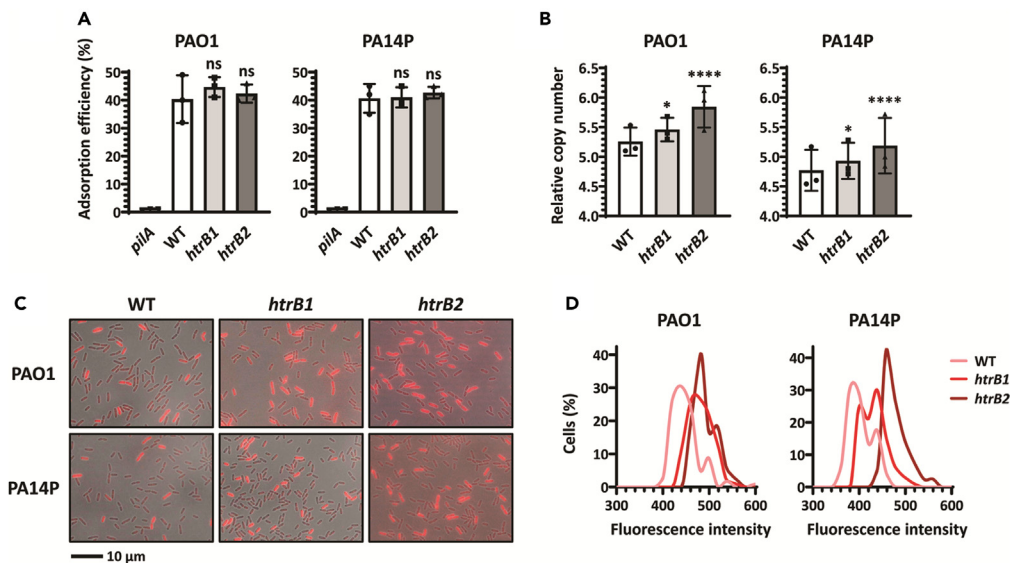
**Figure 3. HtrB2 function in PP7 life cycle**

(A) Phage adsorption assay with PP7. Phage lysates were incubated with the wild type (WT) or one of the isogenic mutants (*pilA*, *htrB1*, and *htrB2*) in either PAO1 or PA14P background. Unbound phages in the supernatant were measured by plaque assay to calculate the adsorption efficiency. The values are from the three biological replicates and the error bars represent the standard deviations. Statistical significance based on Student's *t* test: ns, not significant.

(B) The genomic RNA levels assessed by RT-qPCR immediately after infection. Both the WT and one of the isogenic mutants (*htrB1* and *htrB2*) in either PAO1 or PA14P backgrounds were infected by PP7. The RNA levels from the infected cells were analyzed by RT-qPCR at 30 min post-infection and the PP7 RNA levels were calculated from the standard curve and the relative values with the *rpoA* mRNA levels as the internal controls are designated. A base-10 logarithmic (log) scale is used for the y axis with standard errors from three biological replicates. Statistical significance based on Student's *t* test: *, $p < 0.05$; ****, $p < 0.001$; ns, not significant.

(C) The genomic RNA levels immediately after infection assessed by FISH. The representative fluorescence images are overlapped with the corresponding bright field images from three independent biological replicates. Both the WT and one of the isogenic mutants (*htrB1* and *htrB2*) in either PAO1 or PA14P backgrounds were infected by PP7 as in B. After 30-min incubation, cells were analyzed by FISH as described in method details. The scale bar (10 μm) is designated at the bottom.

(D) The fluorescence intensities were quantified from about 1,000 cells from FISH fields as in C and the frequencies were designated.

PAO1. This might be associated with the differences in the OM integrity of PAO1 and PA14P regarding vancomycin uptake. It should be noted again that HtrB2 is largely the major contributor to the lipid A acylation-mediated antibiotic resistance. Collectively, we suggest that the lipid A acylation-directed OM integrity might be crucial in thwarting the uptake of RNA phages and some antibiotics, as a physical barrier in PA strains.

### Chemical-mediated increase of OM permeability affects the PP7 infectivity

To investigate the roles of the lipid A acylation-directed OM integrity in thwarting RNA phage infection, we hypothesized that the treatment of chemicals affecting the OM permeability might mimic the *htrB* mutant phenotypes observed in the PA cells. To this end, we exploited PMB, a cyclic cationic peptide antimicrobial that directly interacts with the lipid A acyl chains of the OM via ionic and hydrophobic interactions.[22,23] Based on the measured minimum inhibitory conectration (MIC) values of PMB against PA strains under various conditions,[24] we examined whether the PAO1, PA14P, and another PP7-susceptible strain, PMM49[14] might display enhanced PP7 susceptibility in liquid culture or plate culture by subinhibitory concentrations of PMB (i.e., 1.0 μg/mL for broth and 20 ng/mL for plate). Figure 5A shows that PMB treatment enhanced the PP7 susceptibility in three PA strains, whose basal susceptibilities appeared to differ. Furthermore, the PMB treatment clearly enlarged the plaque size on plates only for PP7, not for the TFP-specific DNA phages (MPK7 and MP29) (Figures 5B and 5C). This result substantiates the OM integrity would be a critical component in RNA phage infection, and, more importantly, that the differential OM integrity of diverse PA strains may function as another barrier for RNA phage infectivity.

### Temperature-mediated alteration of OM permeability affects the PP7 infectivity

Since the *htrB2*-mediated OM integrity is important for the growth especially at low temperature,[17] which might be prone to lower the OM fluidity, we hypothesized that PP7-susceptibility might be affected also by temperature changes. We measured the cell growth in the presence of PP7 at 25°C or 42°C. As shown in Figure 6, the growth of the *htrB2* mutant was hampered at 25°C in both PAO1 and PA14P. The wild-type cells were slightly more susceptible to PP7 infection at 25°C and resistant to PP7 infection at 42°C, although the susceptibility of PAO1 to MPK7 was not affected at all (Figure 6A). We presumed that the adsorption did not differ under the lower and the higher temperature
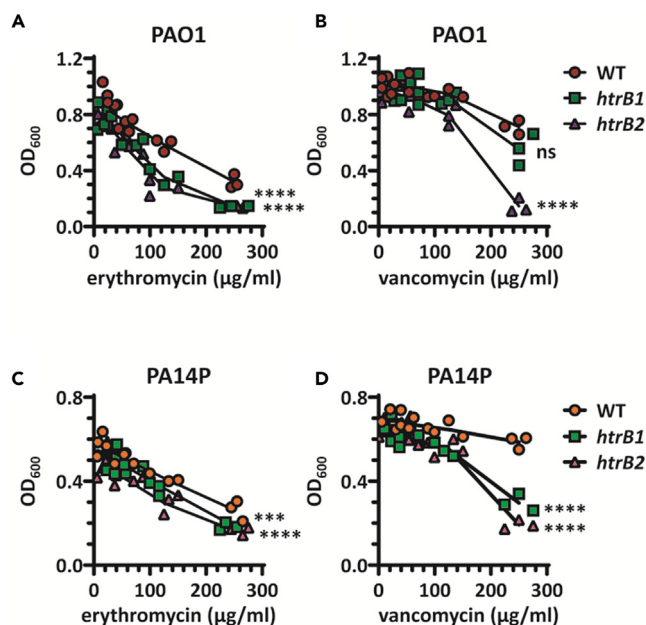
**Figure 4. HtrB2-directed OM permeability change in PAO1 and PA14**

Culture suspensions of the wild type (WT) or one of the isogenic mutants (*htrB1* and *htrB2*) in either PAO1 (A and B) or PA14P (C and D) were inoculated in LB medium containing either erythromycin (A and C) or vancomycin (B and D) at the indicated concentrations and then incubated for 15 h at 37°C. The growth was assessed by measuring the $OD_{600}$ as a function of antibiotic concentrations. Statistical significance based on Dunnett's multiple comparisons test: ***, $p < 0.005$; ****, $p < 0.001$; ns, not significant.

conditions. It is noted that the growth of the *htrB2* mutant was restored at 42°C, with the PP7-resistance in both PAO1 and PA14P. Because elevated temperature *per se* might increase the physical OM fluidity, the cells may have some adaptive or compensatory responses to preserve the proper OM fluidity. This response may obviate the impact of the *htrB2* mutation (i.e., the loss of a secondary acyl chain), in that the acyl chains are in favor of increasing the hydrophobic interactions and thus decreasing the OM fluidity. This result suggests again that the maintenance of proper OM fluidity might be associated with the RNA phage susceptibility.

## DISCUSSION

Lipid A is a glucosamine disaccharide with four primary (*R*)-3-hydroxyacyl chains linked directly to the 2, 3, 2′, and 3′ positions,[25] which also contains phosphate at the 1 and 4′ positions. The hydrophobic lipid A acyl chains sandwiched between the hydrophilic groups function as the membrane anchor[26,27] and thus the hydrophobic interactions between acyl chains of the lipid A presumably determines the structural rigidity of the OM in the Gram-negative bacteria.[28,29] Impairment in lipid A secondary acylation has been shown to alter membrane remodeling in several bacterial species. For example, disruption of *htrB* in *Escherichia coli* inhibited the growth above 33°C, resulting in filamentous or bulging morphology,[30] increased antibiotic susceptibility[31] and decreased capability to colonize human airway epithelium.[32] In case of PA, which harbors two *htrB* genes (*htrB1* and *htrB2*), lipid A secondary acylation is crucial to survive the stressful environmental conditions:[33] the *htrB2* and, to the lesser extent, the *htrB1* mutants displayed increased membrane permeability, and increased chemical susceptibility to some antibiotics and cationic antimicrobial peptides, suggesting a role of these enzymes in maintaining the OM organization and integrity in PA as well. However, a little is known about the involvement of the OM integrity in the phage resistance, despite the potential contribution of the OM remodeling in the uptake of the chemicals and macromolecules.[34,35]

It is most probable that the OM integrity requires the hydrophobic interactions between the acyl chains of lipid A to ensure the physical rigidity as the first-line mechanical barrier to the environmental substances.[36] The impairment of such interactions derived from the *htrB* mutations may affect the physical rigidity and thus compromise the barrier function of the OM for the macromolecules. Considering the average length of van der Walls interactions (∼0.3 nm), the average distance between membrane lipids (∼1 nm) and the Stoke's radius of vancomycin (0.748 nm),[37,38] the disruption of the hydrophobic interactions between the lipid A acyl chains might enhance the fluidity of the OM and thus allow the entry of the antibiotic chemicals. More complex interactions additionally involving electrostatic ones between the OM and the environmental substances at the bacterial surfaces might govern the physicochemical barrier for the phage virions or phage nucleic acids. In that the fiersphage virions are relatively small (∼27 nm) and the injecting genome is a small and flexible RNA molecule, it is hypothesized that the peptidoglycan might not be a critical barrier for the RNA phages, unlike the tailed DNA phages with complex geometry. This hypothesis is also substantiated by the lack of peptidoglycan degradation for the RNA phages during the phage entry as well as phage release.[39] Although it is not yet precisely determined for the PA peptidoglycan, relatively large holes (10–25 nm in diameter) were identified on older
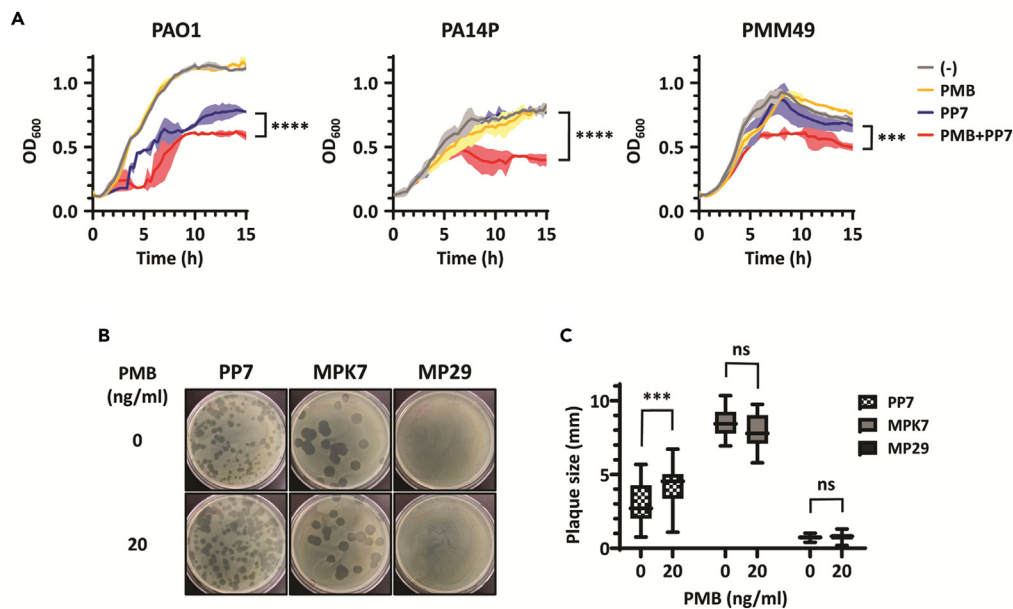
**Figure 5. Chemical-mediated OM permeability in PP7 infectivity**

(A) PMB treatment on PP7 infection. Culture suspensions of *P. aeruginosa* strains (PAO1, PA14P, and PMM49) were mixed with polymyxin B (PMB, 1 mg/mL) and/ or PP7 (at MOI of 10) in LB medium and then incubated further at 37°C. The growth was assessed by measuring the $OD_{600}$ at every 20 min for 15 h. Statistical significance based on Dunnett's multiple comparisons test: ***, $p < 0.005$; ****, $p < 0.001$.

(B) PMB treatment on PP7 plaque phenotypes. Plaques of PP7, MPK7, or MP29 were investigated on the PAO1 lawns in the presence of PMB (20 ng/mL).

(C) PMB treatment on plaque size distribution. The size distribution of the plaques in B is determined and designated using Boxplot. Statistical significance based on unpaired *t*-test: ***, $p < 0.005$; ns, not significant.

regions of the *Staphylococcus aureus* peptidoglycan,[40] which would work as an additional barrier only for the DNA phages with complex geometry. It is more important for the future study to investigate the presumable interplay between the cell wall components and the inner membrane in the differential phage infectivity of PA strains.

It needs to be further verified how HtrB2 would be the major contributor to the phage resistance, while HtrB1 might play a minor role, which was more clearly observed in PA14P rather than in PAO1. This result might be attributed to the fact that the secondary acyl chains might differ in their chemical compositions depending on the PA strains, which accounts for the differential susceptibilities of the PA strains to the RNA phages as well as chemical antibiotics. A deeper understanding into the roles of lipid A acylation in various PA strains might help treat the more complicated infections caused by various PA clones in clinical settings.

## Limitations of the study

Our study does not allow us to conclude that lipid A profiles have differentially evolved to prevent RNA phage entry in various PA strains, but the fact that secondary acyl chains in lipid A might affect the OM integrity in PA strains suggests that PA strains may quantitatively differ in the OM integrity. Further work would be necessary to figure out if the basal OM integrity would differ from strain to strain and how the differences in the OM integrity might influence the RNA phage susceptibility under various circumstances as well as in the clinical settings. In addition, we hypothesize that it is genomic RNA molecules rather than phage particles that pass the OM layer and enter the cytoplasm after adsorption of phage particles to TFPs. To shed further light on this hypothesis, the phage materials could be analyzed by genetic dissection of the maturation protein functions as well as high-resolution microscopies.

## STAR★METHODS

Detailed methods are provided in the online version of this paper and include the following:

- KEY RESOURCES TABLE
- RESOURCE AVAILABILITY
  - Lead contact
  - Materials availability
  - Data and code availability
- EXPERIMENTAL MODEL AND STUDY PARTICIPANT DETAILS
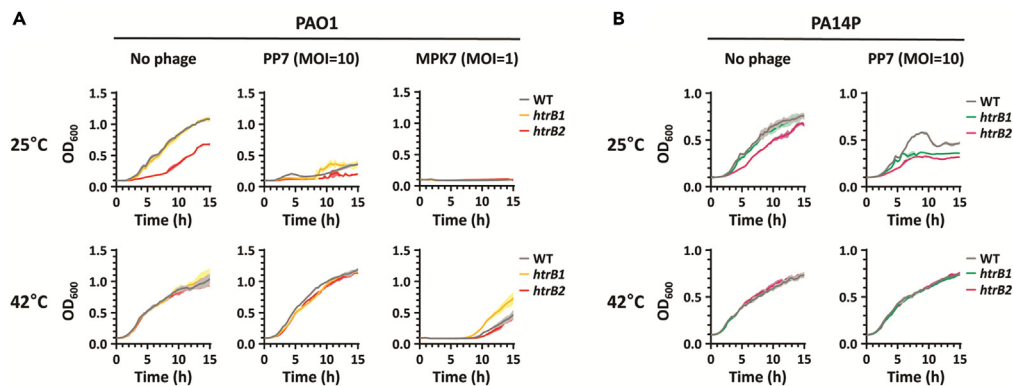- METHOD DETAILS

**Figure 6. Temperature and PP7 infectivity**

(A and B) Growth curve of the *htrB1* and *htrB2* deletion mutants at 25°C and 42°C. Culture suspensions of the wild type (WT) or the isogenic mutants (*htrB1* and *htrB2*) of PAO1 (A) and PA14P (B) were mixed with the phage lysates of either PP7 (at MOI of 10) or MPK7 (at MOI of 1) in LB medium and then incubated further at either 25°C or 42°C. The growth was assessed by measuring the $OD_{600}$ at every 20 min for 15 h.

○ Preparation of phage lysates
○ Phage infection assay
○ Twitching motility assay
○ Isolation of transposon mutants
○ Construction of mutants
○ Phage adsorption assay
○ RNA assay
○ Fluorescence *in situ* hybridization
○ Antibiotic susceptibility assay
● QUANTIFICATION AND STATISTICAL ANALYSIS

## SUPPLEMENTAL INFORMATION

Supplemental information can be found online at https://doi.org/10.1016/j.isci.2023.108675.

## AUTHOR CONTRIBUTIONS

H.-W.B. and Y.-H.C. conceived and designed the research. H.-W.B. and S.-Y.C. designed and performed the experiments, and collected and analyzed the experimental data. H.-W.B. and Y.-H.C. wrote the manuscript. All authors reviewed the manuscript.

## DECLARATION OF INTERESTS

The authors declare no competing interests.

## REFERENCES

1. Ackerman, H.W., and DuBow, M.S. (1987). Viruses of Prokaryotes (General Properties of Bacteriophages), pp. 49–85.
2. Hyman, P., and Abedon, S.T. (2010). Bacteriophage host range and bacterial resistance. Adv. Appl. Microbiol. *70*, 217–248.
3. Dupuis, M.È., Villion, M., Magadán, A.H., and Moineau, S. (2013). CRISPR-Cas and restriction–modification systems are compatible and increase phage resistance. Nat. Commun. *4*, 2087.
4. Price, V.J., Huo, W., Sharifi, A., and Palmer, K.L. (2016). CRISPR-Cas and restriction-modification act additively against conjugative antibiotic resistance plasmid transfer in *Enterococcus faecalis*. mSphere *1*, e00064-16.
5. Oechslin, F., Piccardi, P., Mancini, S., Gabard, J., Moreillon, P., Entenza, J.M., Resch, G., and Que, Y.A. (2017). Synergistic interaction between phage therapy and antibiotics clears *Pseudomonas aeruginosa* infection in

endocarditis and reduces virulence. J. Infect. Dis. *215*, 703–712.

6. Chan, B.K., Sistrom, M., Wertz, J.E., Kortright, K.E., Narayan, D., and Turner, P.E. (2016). Phage selection restores antibiotic sensitivity in MDR *Pseudomonas aeruginosa*. Sci. Rep. *6*, 26717.

7. Lu, T.K., and Koeris, M.S. (2011). The next generation of bacteriophage therapy. Curr. Opin. Microbiol. *14*, 524–531.

8. Kortright, K.E., Chan, B.K., Koff, J.L., and Turner, P.E. (2019). Phage therapy: a renewed approach to combat antibiotic-resistant bacteria. Cell Host Microbe *25*, 219–232.

9. Heo, Y.J., Chung, I.Y., Choi, K.B., Lau, G.W., and Cho, Y.H. (2007). Genome sequence comparison and superinfection between two related *Pseudomonas aeruginosa* phages, D3112 and MP22. Microbiology *153*, 2885–2895.

10. Chung, I.Y., Bae, H.W., Jang, H.J., Kim, B.O., and Cho, Y.H. (2014). Superinfection exclusion reveals heteroimmunity between *Pseudomonas aeruginosa* temperate phages. J. Microbiol. *52*, 515–520.

11. Chung, I.Y., Jang, H.J., Bae, H.W., and Cho, Y.H. (2014). A phage protein that inhibits the bacterial ATPase required for type IV pilus assembly. Proc. Natl. Acad. Sci. USA *111*, 11503–11508.

12. Wang, W., Li, Y., Tang, K., Lin, J., Gao, X., Guo, Y., and Wang, X. (2022). Filamentous prophage capsid proteins contribute to superinfection exclusion and phage defence in *Pseudomonas aeruginosa*. Environ. Microbiol. *24*, 4285–4298.

13. Nguyen, Y., Jackson, S.G., Aidoo, F., Junop, M., and Burrows, L.L. (2010). Structural characterization of novel *Pseudomonas aeruginosa* type IV pilins. J. Mol. Biol. *395*, 491–503.

14. Kim, E.S., Bae, H.W., and Cho, Y.H. (2018). A pilin region affecting host range of the *Pseudomonas aeruginosa* RNA phage, PP7. Front. Microbiol. *9*, 247.

15. Berry, J.L., Xu, Y., Ward, P.N., Lea, S.M., Matthews, S.J., and Pelicic, V. (2016). A comparative structure/function analysis of two type IV pilin DNA receptors defines a novel mode of DNA binding. Structure *24*, 926–934.

16. Chung, I.Y., Kim, Y.K., and Cho, Y.H. (2014). Common virulence factors for *Pseudomonas tolaasii* pathogenesis in *Agaricus* and *Arabidopsis*. Res. Microbiol. *165*, 102–109.

17. Hittle, L.E., Powell, D.A., Jones, J.W., Tofigh, M., Goodlett, D.R., Moskowitz, S.M., and Ernst, R.K. (2015). Site-specific activity of the acyltransferases HtrB1 and HtrB2 in *Pseudomonas aeruginosa* lipid A biosynthesis. Pathog. Dis. *73*, ftv053.

18. Ruokoranta, T.M., Grahn, A.M., Ravantti, J.J., Poranen, M.M., and Bamford, D.H. (2006). Complete genome sequence of the broad host range single-stranded RNA phage PRR1 places it in the *Levivirus* genus with characteristics shared with alloleviviruses. J. Virol. *80*, 9326–9330.

19. Nikaido, H. (2003). Molecular basis of bacterial outer membrane permeability revisited. Microbiol. Mol. Biol. Rev. *67*, 593–656.

20. Ruiz, N., Kahne, D., and Silhavy, T.J. (2006). Advances in understanding bacterial outer-membrane biogenesis. Nat. Rev. Microbiol. *4*, 57–66.

21. Vaara, M., and Nurminen, M. (1999). Outer membrane permeability barrier in *Escherichia coli* mutants that are defective in the late acyltransferases of lipid A biosynthesis. Antimicrob. Agents Chemother. *43*, 1459–1462.

22. Paracini, N., Clifton, L.A., Skoda, M.W.A., and Lakey, J.H. (2018). Liquid crystalline bacterial outer membranes are critical for antibiotic susceptibility. Proc. Natl. Acad. Sci. USA *115*, E7587–E7594.

23. Velkov, T., Thompson, P.E., Nation, R.L., and Li, J. (2010). Structure−activity relationships of polymyxin antibiotics. J. Med. Chem. *53*, 1898–1916.

24. Kim, B.O., Jang, H.J., Chung, I.Y., Bae, H.W., Kim, E.S., and Cho, Y.H. (2021). Nitrate respiration promotes polymyxin B resistance in *Pseudomonas aeruginosa*. Antioxid. Redox Signal. *34*, 442–451.

25. Vorachek-Warren, M.K., Ramirez, S., Cotter, R.J., and Raetz, C.R.H. (2002). A triple mutant of *Escherichia coli* lacking secondary acyl chains on lipid A. J. Biol. Chem. *277*, 14194–14205.

26. Needham, B.D., and Trent, M.S. (2013). Fortifying the barrier: the impact of lipid A remodeling on bacterial pathogenesis. Nat. Rev. Microbiol. *11*, 467–481.

27. Munford, R.S., and Varley, A.W. (2006). Shield as signal: lipopolysaccharides and the evolution of immunity to gram-negative bacteria. PLoS Pathog. *2*, e67.

28. Arunmanee, W., Pathania, M., Solovyova, A.S., Le Brun, A.P., Ridley, H., Baslé, A., van den Berg, B., and Lakey, J.H. (2016). Gram-negative trimeric porins have specific LPS binding sites that are essential for porin biogenesis. Proc. Natl. Acad. Sci. USA *113*, E5034–E5043.

29. Rutten, L., Geurtsen, J., Lambert, W., Smolenaers, J.J.M., Bonvin, A.M., de Haan, A., van der Ley, P., Egmond, M.R., Gros, P., and Tommassen, J. (2006). Crystal structure and catalytic mechanism of the LPS 3-O-deacylase PagL from *Pseudomonas aeruginosa*. Proc. Natl. Acad. Sci. USA *103*, 7071–7076.

30. Karow, M., Fayet, O., Cegielska, A., Ziegelhoffer, T., and Georgopoulos, C. (1991). Isolation and characterization of the *Escherichia coli htrB* gene, whose product is essential for bacterial viability above 33°C in rich media. J. Bacteriol. *173*, 741–750.

31. Karow, M., and Georgopoulos, C. (1992). Isolation and characterization of the *Escherichia coli msbB* gene, a multicopy suppressor of null mutations in the high-temperature requirement gene *htrB*. J. Bacteriol. *174*, 702–710.

32. Swords, W.E., Chance, D.L., Cohn, L.A., Shao, J., Apicella, M.A., and Smith, A.L. (2002). Acylation of the lipooligosaccharide of *Haemophilus influenzae* and colonization: an *htrB* mutation diminishes the colonization of human airway epithelial cells. Infect. Immun. *70*, 4661–4668.

33. Liang, Y., Guo, Z., Gao, L., Guo, Q., Wang, L., Han, Y., Duan, K., and Shen, L. (2016). The role of the temperature-regulated acyltransferase (PA3242) on growth, antibiotic resistance and virulence in *Pseudomonas aeruginosa*. Microb. Pathog. *101*, 126–135.

34. Delcour, A.H. (2009). Outer membrane permeability and antibiotic resistance. Biochim. Biophys. Acta *1794*, 808–816.

35. Guest, R.L., and Raivio, T.L. (2016). Role of the Gram-negative envelope stress response in the presence of antimicrobial agents. Trends Microbiol. *24*, 377–390.

36. Escribá, P.V., González-Ros, J.M., Goñi, F.M., Kinnunen, P.K.J., Vigh, L., Sánchez-Magraner, L., Fernández, A.M., Busquets, X., Horváth, I., and Barceló-Coblijn, G. (2008). Membranes: a meeting point for lipids, proteins and therapies. J. Cell Mol. Med. *12*, 829–875.

37. Song, Q., Cheng, Z., Kariuki, M., Hall, S.C.L., Hill, S.K., Rho, J.Y., and Perrier, S. (2021). Molecular self-assembly and supramolecular chemistry of cyclic peptides. Chem. Rev. *121*, 13936–13995.

38. Eggeling, C., Ringemann, C., Medda, R., Schwarzmann, G., Sandhoff, K., Polyakova, S., Belov, V.N., Hein, B., von Middendorff, C., Schönle, A., and Hell, S.W. (2009). Direct observation of the nanoscale dynamics of membrane lipids in a living cell. Nature *457*, 1159–1162.

39. Labrie, S.J., Samson, J.E., and Moineau, S. (2010). Bacteriophage resistance mechanisms. Nat. Rev. Microbiol. *8*, 317–327.

40. Touhami, A., Jericho, M.H., and Beveridge, T.J. (2004). Atomic force microscopy of cell growth and division in *Staphylococcus aureus*. J. Bacteriol. *186*, 3286–3295.

41. Lee, J.Y., Ahn, S.J., Park, C., Bae, H.W., Kim, E.S., and Cho, Y.H. (2019). Reverse genetic systems for *Pseudomonas aeruginosa* leviphages. Methods Protoc. *2*, 22.

42. Goodman, A.L., Kulasekara, B., Rietsch, A., Boyd, D., Smith, R.S., and Lory, S. (2004). A signaling network reciprocally regulates genes associated with acute infection and chronic persistence in *Pseudomonas aeruginosa*. Dev. Cell *7*, 745–754.

43. Chung, I.Y., Kim, B.O., Jang, H.J., and Cho, Y.H. (2016). Dual promoters of the major catalase (KatA) govern distinct survival strategies of *Pseudomonas aeruginosa*. Sci. Rep. *6*, 31185.

44. Kim, E.S., Lee, J.Y., Park, C., Ahn, S.J., Bae, H.W., and Cho, Y.H. (2021). cDNA-Derived RNA phage assembly reveals critical residues in the maturation protein of the *Pseudomonas aeruginosa* leviphage PP7. J. Virol. *95*, e01643-20.

# STAR★METHODS

## KEY RESOURCES TABLE

| REAGENT or RESOURCE | SOURCE | IDENTIFIER |
|---|---|---|
| **Bacterial and virus strains** | | |
| *Pseudomonas aeruginosa* PAO1 | Laboratory strain | N/A |
| *P. aeruginosa* PA14 | Laboratory strain | N/A |
| *P. aeruginosa* PA14P | This paper | N/A |
| *P. aeruginosa* PA14P 1A8 | This paper | N/A |
| *P. aeruginosa* PA14P 28B11 | This paper | N/A |
| *P. aeruginosa* PAO1 *htrB1* | This paper | N/A |
| *P. aeruginosa* PAO1 *htrB2* | This paper | N/A |
| *P. aeruginosa* PA14P *htrB1* | This paper | N/A |
| *P. aeruginosa* PA14P *htrB2* | This paper | N/A |
| *P. aeruginosa* PAK | Laboratory strain | N/A |
| *P. aeruginosa* PMM49 | Kim et al.[14] | N/A |
| *Escherichia coli* DH5α | Laboratory strain | N/A |
| *E. coli* S17-1 | Laboratory strain | N/A |
| *E. coli* S17-1($\lambda pir$)(pBTK30) | Laboratory strain | N/A |
| *Pseudomonas* phage PP7 | Laboratory strain | N/A |
| *Pseudomonas* phage MPK7 | Laboratory strain | N/A |
| *Pseudomonas* phage MP29 | Laboratory strain | N/A |
| *Pseudomonas* phage PRR1 | Laboratory strain | N/A |
| **Chemicals, peptides, and recombinant proteins** | | |
| Polyethylene glycol | Sigma-Aldrich | 202452 |
| DNase I, RNase-free | Thermo Scientific™ | EN0521 |
| T4 DNA Polymerase | Enzynomics | DP004 |
| Polymyxin B | Sigma-Aldrich | P4932 |
| **Critical commercial assays** | | |
| RNeasy Mini Kit | Qiagen | 74104 |
| RNase-Free DNase Set | Qiagen | 79254 |
| ReverTra Ace™ qPCR RT Kit | TOYOBO | FSQ-201 |
| THUNDERBIRD™ SYBR™ qPCR Mix | TOYOBO | QPS-201 |
| **Oligonucleotides** | | |
| Primers and probes, see Table S1 | This paper | N/A |
| **Recombinant DNA** | | |
| Plasmid: pEX18T | Laboratory stock | N/A |
| pEX18T-pilA$_{O1}$ | This paper | N/A |
| pEX18T-htrB1 | This paper | N/A |
| pEX18T-htrB2 | This paper | N/A |
| **Software and algorithms** | | |
| Excel (version 2310) | Microsoft | N/A |
| ZEN 2.6 (blue edition) | Carl Zeiss Microscopy | RRID:SCR_013672 |
| Prism 5.0 | GraphPad | RRID:SCR_002798 |
| ImageJ (version 1.8.0) | https://imagej.nih.gov | RRID:SCR_003070 |

## RESOURCE AVAILABILITY

### Lead contact

Further information and requests for resources and reagents should be directed to and will be fulfilled by the lead contact, You-Hee Cho (youhee@cha.ac.kr).

### Materials availability

This study did not generate new unique reagents.

### Data and code availability

- Data reported in this study will be shared by the lead contact (youhee@cha.ac.kr) upon request.
- This study does not report original code.
- Any additional information required to reanalyze the data reported in this study is available from the lead contact (youhee@cha.ac.kr) upon request.

## EXPERIMENTAL MODEL AND STUDY PARTICIPANT DETAILS

*Pseudomonas aeruginosa* (PAO1, PA14, PAK, and PMM49) and *Escherichia coli* (DH5α, S17-1, and S17-1(λ*pir*)) strains were used in this study, with their relevant information described elsewhere.[24] Bacterial cells were grown at 37°C using Luria-Bertani (LB) broth or onto 2% Bacto-agar (Difco) LB plates. Cetrimide agar (Difco) plates were used for selection of *P. aeruginosa* strains. Antibiotics were amended in the following concentrations (μg/ml): for *P. aeruginosa*, gentamicin (50), and carbenicillin (200); for *E. coli*, gentamicin (25) and ampicillin (50).

## METHOD DETAILS

### Preparation of phage lysates

Phage lysates of MPK7, MP29, and PRR1 were prepared by plate lysate method, using *P. aeruginosa* strain PAO1, while PP7 lysates were prepared using PAK cells containing the PP7 cDNA that had been cultured in 200 ml LB broth for 24 h at 30°C as described elsewhere.[41] Phage particles were precipitated with 1M NaCl and 10% polyethylene glycol (average molecular weight, 8,000 Da) (Sigma-Aldrich) at 4°C overnight, pelleted by centrifugation, and dissolved in phage buffer (100 mM NaCl, 50 mM Tris [pH7.5], 10 mM MgSO$_4$, 1 mM EDTA) (5 ml). Phage particles were further concentrated by ultracentrifugation at 100,000 × *g* for 3 h and then resuspended in phage buffer (1 ml). The plaque forming unit (PFU) of the phage lysates were determined prior to being used.

### Phage infection assay

Phage infection was performed either in the liquid cultures or on the plate cultures of *P. aeruginosa* cells as described previously.[14] For liquid cultures, bacterial growth was assessed spectrophotometrically in the presence of phages at the designated multiplicity of infection (MOI) by measuring the optical density at 600 nm (OD$_{600}$) using a microplate reader (BioTek Epoch2). For plate cultures, droplets (3 μl) of serially diluted phage samples were spotted onto the lawns of *P. aeruginosa* cells (50 μl) from the late-exponential-phase cultures. The plates were incubated at 37°C for 16 h. Alternatively, 3 μl of the phage samples was mixed with 3 ml top agar containing $10^8$ cells of *P. aeruginosa* cells and then the mixture was plated onto LB agar. Phage plaques were examined after 16-h incubation at 37°C. Polymyxin B was used to disrupt the OM integrity.

### Twitching motility assay

A single colony from overnight culture on LB agar plates was picked with a toothpick and stabbed to the bottom of a 3-mm thick 1.5% LB agar plate.[14] A twitching zone at the interface between the agar and the bottom of the plates was visualized by staining with 0.1% crystal violet after 24-h incubation at 30°C.

### Isolation of transposon mutants

Random transposon mutagenesis was performed by using pBTK30, containing a *mariner*-based transposon.[42] Biparental mating from *E. coli* S17-1(λ*pir*) harboring pBTK30 to *P. aeruginosa* PA14P (see below) was performed onto LB agar plates for 6 h at 37°C. Selection and counterselection was done using cetrimide agar plates containing 50 μg/ml gentamicin. A total of 31,474 insertion clones were screened for the mutants exhibiting retarded growth in the presence of PP7 to isolate 283 primary candidates. Among the 12 clones after secondary screening, the transposon insertion sites of 10 clones were determined by arbitrary PCR followed by sequencing as described elsewhere[16] using the primers (Table S1).

### Construction of mutants

PA14P is a PA14 derivative whose *tfpY-pilA* region between *pilB* and tRNA$^{Thr}$ had been replaced with the corresponding region from PAO1 based on 6-primer SOEing (splicing by overlap extension) PCR (Table S1). The lipid A-defective mutants for either *htrB1* or *htrB2* mutants were

created by 4-primer SOEing PCR in both PAO1 and PA14P backgrounds. The double-crossover mutants were generated by using pEX18T-based allelic exchange as described elsewhere.[43] PA14P and the deletion mutants were verified by PCR and phenotypic assays (if applicable).

### Phage adsorption assay

Phage adsorption was enumerated as described previously.[14] Briefly, PAO1 bacteria including the isogenic *pilA* mutant as the negative control were grown on tryptic soy (TS) agar plates at 37°C for 16 h, and ~$10^8$ bacterial cells were resuspended in 500 μl TS broth. PP7 of $3 \times 10^7$ PFU was added and allowed to adsorb to the cells at 37°C for 5 min. The resulting phage-cell complex was pelleted at $500 \times g$ for 10 min at 4°C to remove the bound phages and the PFU of the recovered supernatant containing unbound phages was enumerated by plaque assay.

### RNA assay

PP7 genome synthesis in the infected cells was measured by real-time PCR (qPCR) following reverse transcription (RT) as described elsewhere.[44] Briefly, PAO1 cells were inoculated in LB, grown at 37°C to late-exponential phase (i.e., $OD_{600}$ of 1), centrifuged at $10,000 \times g$ for 10 min, and resuspended in 50 μl LB. PP7 phages were added at MOI of 0.1 and allowed to adsorb to the cells at 37°C for 5 min. The phage-cell complex was transferred to 10 ml LB and cultured at 37°C for 30 min. The cells were harvested for RNA extraction using a RNeasy mini kit (Qiagen), according to the manufacturer's instructions. The RNA samples were subjected to DNase I digestion (Qiagen) and subjected to RT-qPCR using primers (Table S1) and the StepOnePlus qPCR system (Applied Biosystems). The copy numbers of PP7 genome relative to those of *rpoA* were calculated using standard curves of each gene.

### Fluorescence *in situ* hybridization

Phage genome synthesis was enumerated by fluorescence *in situ* hybridization (FISH). Briefly, PAO1 cells that had been grown at 37°C to $OD_{600}$ of 1.0 were harvested at $10,000 \times g$ for 10 min and resuspended in 50 μl LB. PP7 phages were added at MOI of 10 and allowed to adsorb to the cells at 37°C for 5 min. The phage-cell complex was inoculated 10 ml LB in a baffled flask and cultured at 37°C for 30 min. Aliquots (2 ml) were obtained by centrifugation at $10,000 \times g$ for 5 min and then resuspended in 1 ml PBS (pH 7.4) containing 4% (wt/vol) formaldehyde for 3 h at room temperature. The samples were centrifuged at $10,000 \times g$ for 5 min to obtain the cell pellets, which were subjected to addition of 1 ml of 50% (vol/vol) ethanol and incubation for 5 min at room temperature. After centrifugation, the cell pellets were incubated at 4°C for at least 1 h and then subjected to hybridization using Cy3-labelled PP7-specific probe, PP7-RP-FISH (Table S1) (500 pmol), in 100-μl hybridization solution (20 mM Tris-Cl (pH 8.0), 0.9 M NaCl, 0.01% SDS, 40% formamide) over a shaking incubator at 42°C until complete homogenization of cell pellets is observed (~2 h). After hybridization, cells were washed twice with $0.1 \times$ SSC (saline-sodium citrate) (1 ml), placed on microscopic slides, and observed on a fluorescence microscope (Zeiss Axio Observer Z1). The fluorescence signals were quantified by using Zeiss ZEN.

### Antibiotic susceptibility assay

Antibiotic susceptibility was assessed by growth measurement in the presence of either erythromycin or vancomycin at various concentrations (15.6, 31.3, 62.5, 125, and 250 μg/ml). Briefly, *P. aeruginosa* cells were used to inoculate antibiotic-containing LB broth at $2.0 \times 10^8$ cells/ml in a 96-well microplate and grown at 37°C for 8 h to determine the $OD_{600}$. Three independent cultures were used to measure the antibiotic susceptibility at each antibiotic concentration.

## QUANTIFICATION AND STATISTICAL ANALYSIS

The results are presented as the means with the real data and were analyzed by Dunnett's multiple comparisons tests using GraphPad 5.0 statistical software. For box and whisker plotting, unpaired *t*-tests were performed to analyze one-tailed *p*-value with confidence intervals of 95% as described elsewhere.[24] A *p*-value of less than 0.05 was considered statistically significant.